Electronic Supplementary Material (ESI) for Journal of Materials Chemistry B.

Supplementary Information

On-demand activatable peroxidase-mimicking enzymatic polymer nanocomposite films

Md. Lutful Amin,[a] Ayad Saeed,[b,c] Le N. M. Dinh,[a] Jiachen Yan,[b] Haotian Wen,[b] Shery L. Y. Chang,[b,d] Yin Yao,[d] Per B. Zetterlund,[a] Tushar Kumeria,[b,c,e]* Vipul Agarwal[a]*

[a]*Cluster for Advanced Macromolecular Design (CAMD), School of Chemical Engineering, University of New South Wales, Sydney, NSW 2052, Australia*
[b]*School of Materials Science and Engineering, University of New South Wales, Sydney, NSW 2052, Australia*
[c]*Australian Centre for Nanomedicine, University of New South Wales, Sydney, NSW 2052, Australia*
[d]*Mark Wainwright Analytical Centre, University of New South Wales, Sydney, NSW 2052, Australia*
[e]*School of Pharmacy, University of Queensland, Brisbane, QLD 4102, Australia*

*Corresponding authors: t.kumeria@unsw.edu.au, agarwalvipul84@gmail.com

Table S1: Particle size analyses of iron oxide nanoparticles.

Sample	Average Size (nm)	PDI
Iron oxide nanoparticles	127	0.0556

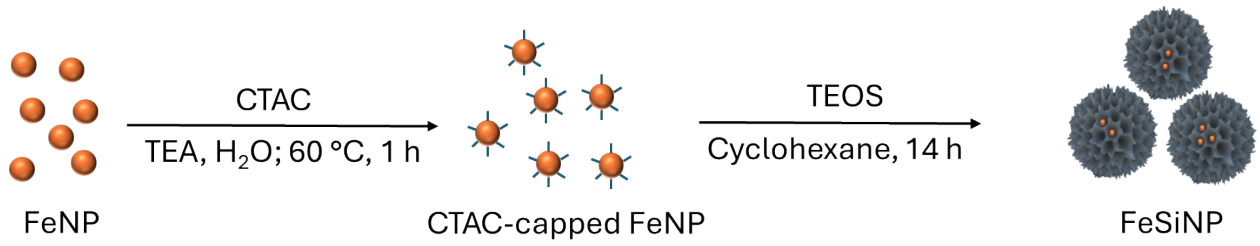

Figure S1. FeSiNP: synthesis of mesoporous silica nanoparticles and decoration with iron oxide nanoparticles.

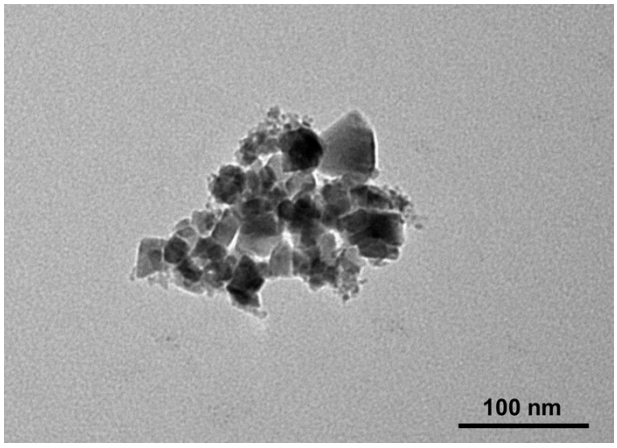

Figure S2. Characterisation of iron oxide nanoparticles by STEM (scale bar = 100 nm).

Table S2: Monomer conversion and particle size analyses of polymer latex.

P(St-*stat*-*n*BA)/FeSiNP	**5 wt%**	**10 wt%**	**20 wt%**
Conversion (%)	85.4	85.4	90.6
Intensity-average particle size (d_i)	85.0	88.9	82.0

Table S3: Molecular weight analyses of polymer latex by GPC.

P(St-*stat*-*n*BA)/FeSiNP	**M_n (g/mol)**	**M_w (g/mol)**	***Đ***
5 wt%	101,132	413,259	4.08
10 wt%	108,325	428,996	3.96
20 wt%	111,999	364,318	3.25

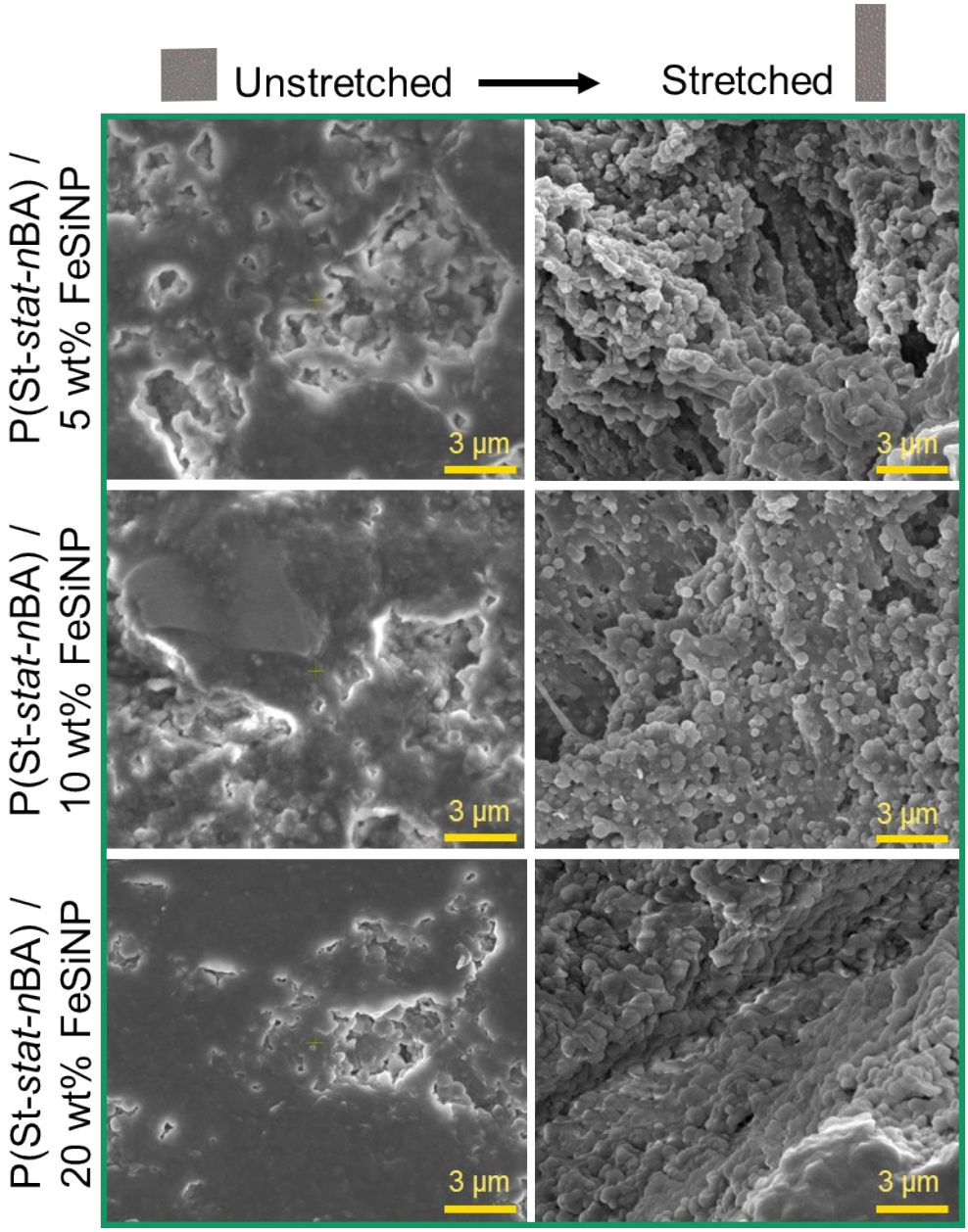

Figure S3. Characterisation of P(St-*stat*-*n*BA)/FeSiNP films – higher magnification SEM images of nanocomposite films under unstretched and stretched conditions showing overall surface features with the presence of spherical FeSiNPs in the crevices (scale bar = 3 µm).

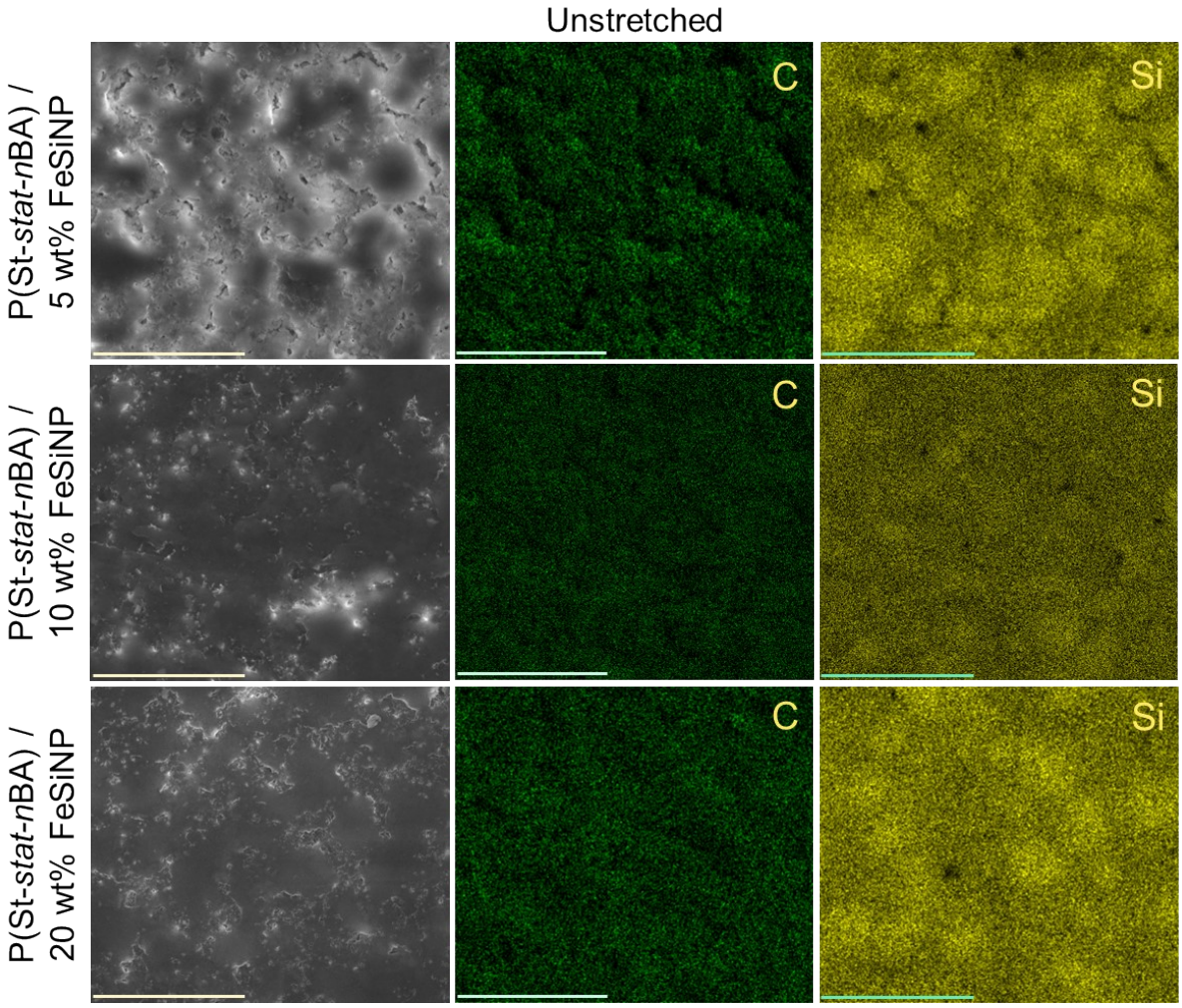

Figure S4. Characterisation of P(St-*stat*-*n*BA)/FeSiNP films- SEM images in unstretched condition and EDS mapping confirming the elements in images (scale bar = 25 µm).

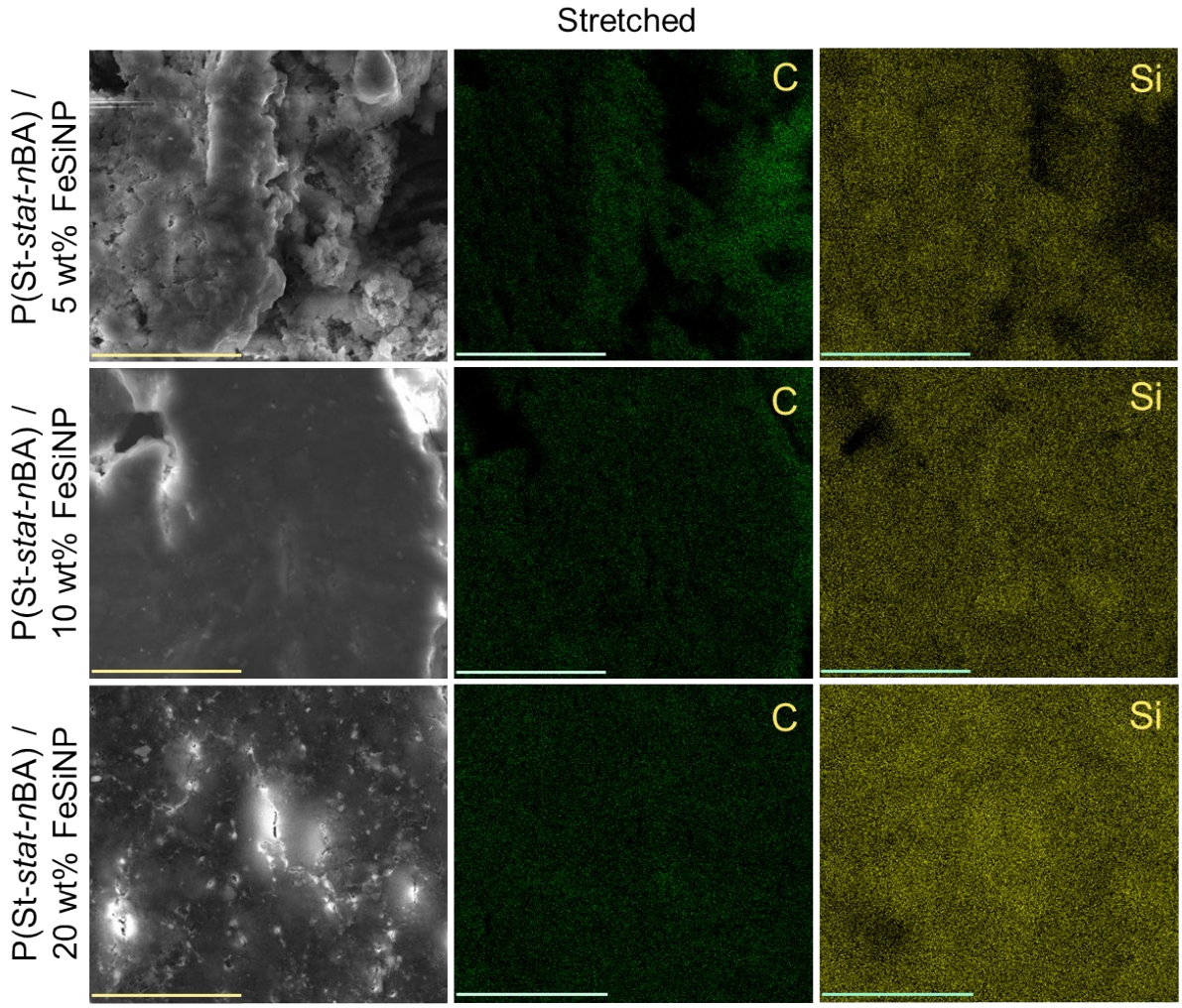

Figure S5. Characterisation of P(St-*stat*-*n*BA)/FeSiNP films- SEM images in stretched condition and EDS mapping confirming the elements in images (scale bar = 25 µm).

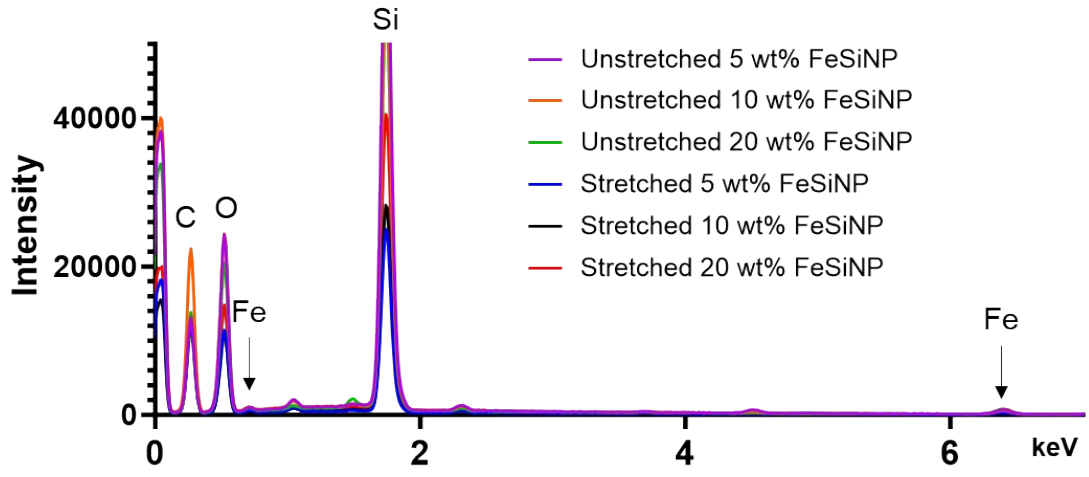

Figure S6. SEM-EDS spectra of the scanned images showing the presence of iron and silicon.

Table S4: Mechanical properties of P(St-*stat*-*n*BA)/FeSiNP nanocomposite films.

NP (wt%)	Film thickness (mm)	Tensile strength (MPa)	Elongation at break (%)
5	58	0.78 ± 0.08	1448
10	62	1.71 ± 0.21	847 ± 27
20	70	1.15 ± 0.09	860 ± 46

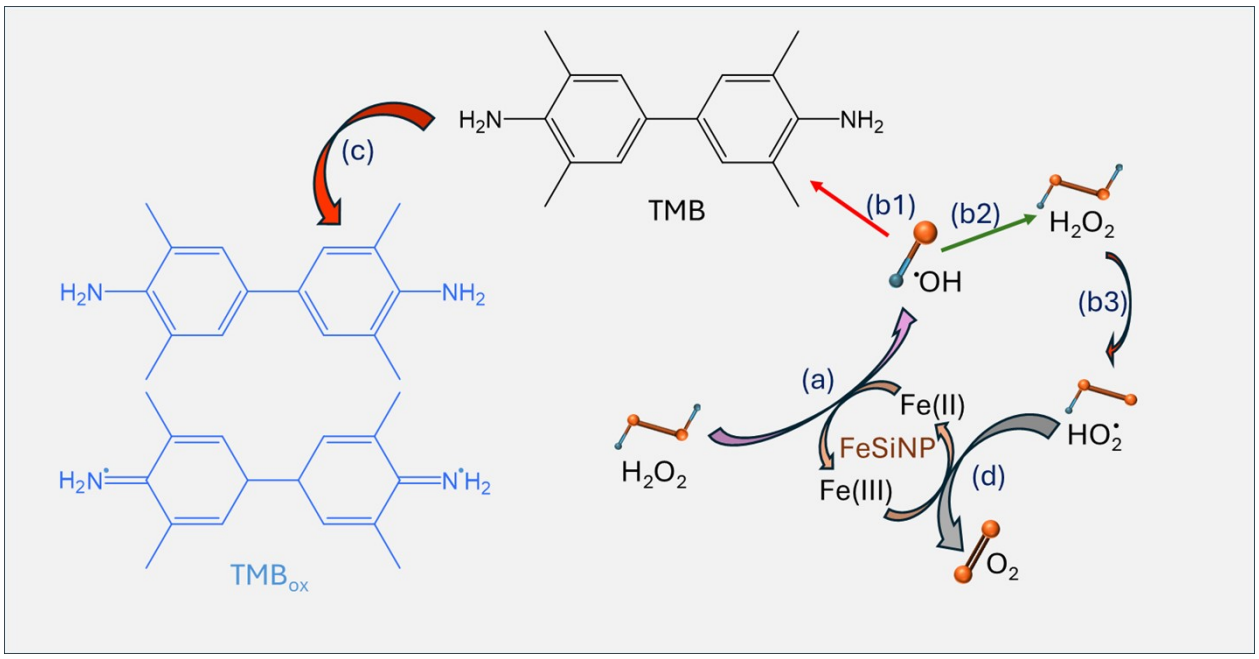

Figure S7. The proposed mechanism of catalytic activity of FeSiNP as adapted from[1].

The equations S1-4 describe the stepwise catalytic mechanism of nanozyme FeSiNPs in this study:

$$Fe^{2+} + H2O2 \rightarrow \cdot OH + Fe^{3+} + H2O \quad \textbf{(S1)}$$

$$\cdot OH + TMB \rightarrow TMBox + H2O \quad \textbf{(S2)}$$

$$\cdot OH + H2O2 \rightarrow HO2\cdot + H2O \quad \textbf{(S3)}$$

$$HO2\cdot + Fe^{3+} \rightarrow Fe^{2+} + O2 \quad \textbf{(S4)}$$

Based on the obtained data in this study and previously published report[1], equation S1 is the rate limiting step.

Table S5: Catalytic parameter comparison among different nanozymes.

NP	Substrate	K_m (mM)	V_{max} (μM/s)	Reference
Ir nanoparticle	H_2O_2	0.27	1.5	[2]
	TMB	-	-	
Au nanocrystal	H_2O_2	16.0	0.452	[3]
	TMB	-	-	

Pt nanoparticle	H_2O_2	41.8	0.167	4
	TMB	0.119	0.21	
Pt nanocrystal	H_2O_2	3.07	0.1817	5
	TMB	0.096	0.1414	
Cu nanocrystal	H_2O_2	29.16	0.0422	6
	TMB	0.648	0.0596	
Pd nanoparticle	H_2O_2	537.71	0.112	7
	TMB	0.09	0.177	
Fe_3O_4 nanoparticle	H_2O_2	10.58	0.1459	8
	TMB	6.22	0.157	
Co_3O_4 nanoparticle	H_2O_2	34.3	11.2	9
	TMB	-	-	
Fe_3O_4-MoS_2 nanoparticle	H_2O_2	1.39	1.63	10
	TMB	0.25	0.111	
Fe_3O_4-C nanowire	H_2O_2	0.23	0.0241	11
	TMB	0.20	0.0134	
Co-dopped Fe_3O_4 nanoparticle	H_2O_2	0.19	0.715	12
	TMB	1.17	0.379	
Fe_2O_3 nanocomposite	H_2O_2	0.885	-	13
	TMB	0.582	-	
Nanocellulose Fe_3O_4/Ag nanoparticle	H_2O_2	8.77	0.107	14
	TMB	0.387	0.133	
FeSiNP (our work)	H_2O_2	0.060	0.00672	
	TMB	7.143	0.01075	

A lower K_m value suggests higher affinity. V_{max} is the maximum rate of conversion into the product.

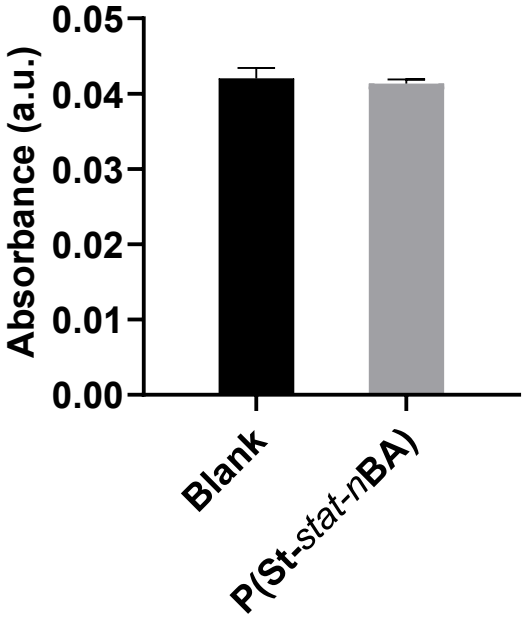

Figure S8. Control experiments – catalytic activity of buffer (blank) and films without FeSiNPs, showing similar absorbance values, which are negligible and considered as a baseline.

References:

1. B. Yuan, H.-L. Chou and Y.-K. Peng, *ACS Appl. Mater. Interfaces*, 2022, **14**, 22728-22736.
2. G. Jin, J. Liu, C. Wang, W. Gu, G. Ran, B. Liu and Q. Song, *Appl. Catal. B*, 2020, **267**, 118725.
3. C.-P. Liu, T.-H. Wu, C.-Y. Liu, K.-C. Chen, Y.-X. Chen, G.-S. Chen and S.-Y. Lin, *Small*, 2017, **13**, 1700278.
4. W. Li, B. Chen, H. Zhang, Y. Sun, J. Wang, J. Zhang and Y. Fu, *Biosens. Bioelectron.*, 2015, **66**, 251-258.
5. L. Jin, Z. Meng, Y. Zhang, S. Cai, Z. Zhang, C. Li, L. Shang and Y. Shen, *ACS Appl. Mater. Interfaces*, 2017, **9**, 10027-10033.
6. L. Hu, Y. Yuan, L. Zhang, J. Zhao, S. Majeed and G. Xu, *Anal. Chim. Acta*, 2013, **762**, 83-86.
7. S.-B. He, F.-Q. Chen, L.-F. Xiu, H.-P. Peng, H.-H. Deng, A.-L. Liu, W. Chen and G.-L. Hong, *Anal. Bioanal. Chem.*, 2020, **412**, 499-506.
8. W. Li, G.-C. Fan, F. Gao, Y. Cui, W. Wang and X. Luo, *Biosens. Bioelectron.*, 2019, **127**, 64-71.
9. J. Mu, L. Zhang, M. Zhao and Y. Wang, *J. Mol. Catal. A Chem.*, 2013, **378**, 30-37.
10. F. Wei, X. Cui, Z. Wang, C. Dong, J. Li and X. Han, *Chem. Eng. J.*, 2021, **408**, 127240.
11. R. Zhang, N. Lu, J. Zhang, R. Yan, J. Li, L. Wang, N. Wang, M. Lv and M. Zhang, *Biosens. Bioelectron.*, 2020, **150**, 111881.
12. Y. Wang, H. Li, L. Guo, Q. Jiang and F. Liu, *RSC Adv.*, 2019, **9**, 18815-18822.
13. X. Liu, T. Gao, H. Liu, Y. Fang and L. Wang, *J. Exp. Nanosci.*, 2022, **17**, 75-85.
14. S. A. Geleto, A. M. Ariti, B. T. Gutema, E. M. Abda, A. A. Abiye, S. M. Abay, M. L. Mekonnen and Y. A. Workie, *ACS Omega*, 2023 **8**, 48764–48774.